

Pullulan-based nanoparticles as carriers for transmucosal protein delivery

Marita Dionísio^{1,2}, Clara Cordeiro^{2,3}, Carmen Remuñán-López,⁴ Begoña Seijo,⁴ Ana M. Rosa da Costa^{2,5}, Ana Grenha^{1,2*}

¹CBME – Centre for Molecular and Structural Biomedicine / IBB – Institute for Biotechnology and Bioengineering, 8005-139 Faro, Portugal; ²Faculty of Sciences and Technology, University of Algarve, Campus de Gambelas, 8005-139 Faro, Portugal; ³CEAUL, Faculty of Sciences, University of Lisbon, Campo Grande, 1749-016 Lisboa, Portugal; ⁴NanoBioFar Group, Department of Pharmacy and Pharmaceutical Technology, Faculty of Pharmacy, University of Santiago de Compostela, Campus Vida, 15782 Santiago de Compostela, Spain; ⁵CIQA –Algarve Chemistry Research Centre, 8005-139 Faro, Portugal

Author e-mails (authorship order): maritadionisio@gmail.com, cmhcordei@gmail.com, mdelcarmen.remunan@usc.es, mbegona.seijo@usc.es, amcosta@ualg.pt, amgrenha@ualg.pt

*Corresponding author:

University of Algarve

CBME/IBB, Faculty of Sciences and Technology

Campus de Gambelas

8005-139 Faro, Portugal

Tel.: +351 289800100 – Ext. 7441

Fax: +351 289818419

E-mail address: amgrenha@ualg.pt

Abstract

Polymeric nanoparticles have revealed very effective in transmucosal delivery of proteins. Polysaccharides are among the most used materials for the production of these carriers, owing to their structural flexibility and propensity to evidence biocompatibility and biodegradability. In parallel, there is a preference for the use of mild methods for their production, in order to prevent protein degradation, ensure lower costs and easier procedures that enable scaling up.

In this work we propose the production of pullulan-based nanoparticles by a mild method of polyelectrolyte complexation. As pullulan is a neutral polysaccharide, sulfated and aminated derivatives of the polymer were synthesized to provide pullulan with a charge. These derivatives were then complexed with chitosan and carrageenan, respectively, to produce the nanocarriers. Positively charged nanoparticles of 180-270 nm were obtained, evidencing ability to associate bovine serum albumin, which was selected as model protein. In PBS pH 7.4, pullulan-based nanoparticles were found to have a burst release of 30% of the protein, which maintained up to 24h. Nanoparticle size and zeta potential were preserved upon freeze-drying in the presence of appropriate cryoprotectants. A factorial design was approached to assess the cytotoxicity of raw materials and nanoparticles by the metabolic test MTT. Nanoparticles demonstrated to not cause overt toxicity in a respiratory cell model (Calu-3). Pullulan has, thus, demonstrated to hold potential for the production of nanoparticles with an application in protein delivery.

Keywords: carrageenan, chitosan, drug delivery, nanoparticles, protein delivery, pullulan

1. Introduction

Finding adequate strategies to deliver proteins has become an urgent scientific challenge, and transmucosal administration is now the first-line option for their systemic delivery. Nanoparticles have been proposed as suitable protein carriers, overcoming many of the limitations posed by the physicochemical characteristics of these macromolecules, which are very susceptible to degradation and undergo difficult absorption due to their size and, usually, hydrophilicity (Antosova et al., 2009; Liu et al., 2008). Nanoparticles potentiate the improvement of drug pharmacokinetic profile, not only by providing their stabilisation but, in some cases, also permitting controlled release and enhancing drug absorption (Grenha, 2012; Hartig et al., 2007). Moreover, the high surface-to-volume ratio displayed by nanoparticles increases drug loading capacity (de la Fuente et al., 2008a). Previous studies have demonstrated that nanoparticle contact with epithelial surfaces is maximised when they display a size within 50 and 500 nm (Desai et al., 1996; Jani et al., 1990) and a strongly positive zeta potential (Bogataj et al., 2003; Carvalho et al., 2010).

Polymers have been referred as the best class of materials to produce nanoparticles and polysaccharides are among the most used (Karewicz et al., 2012; Liu et al., 2008), because their natural origin offers better potential for complying with the requisites of biocompatibility and biodegradability, which are mandatory in the design of drug delivery systems (Beneke et al., 2009; Liu et al., 2008; Malafaya et al., 2007).

Moreover, polysaccharides also exhibit great structural flexibility, forming either linear or branched structures and easily permitting chemical modifications (Karewicz et al., 2012; Malafaya et al., 2007). In recent years, the most frequently explored polysaccharide for the design of nanodelivery systems was chitosan, a cationic polymer composed of repeating β -(1,4)-linked *N*-acetylglucosamine and D-glucosamine units,

which is obtained by **chitin deacetylation and assumes** different molecular weights and deacetylation degrees (Chiellini et al., 2008; Hassani et al., 2012; Mizrahy and Peer, 2012). Apart from the reported biocompatibility and biodegradability (Dornish et al., 1997; Grenha et al., 2010a; Hirano et al., 1988), the most outstanding properties of chitosan rely on its mucoadhesive character (Lehr et al., 1992) and demonstrated ability to potentiate **transmucosal** absorption both as molecule (Artursson et al., 1994; Borchard et al., 1996; Portero et al., 2002) and in the form of nanoparticle (Al-Qadi et al., 2012; De Campos et al., 2001; Fernández-Urrusuno et al., 1999a; Prego et al., 2005a; Yamamoto et al., 2005).

Other polysaccharides integrating the list of “most used” in similar applications are alginate, dextran and hyaluronic acid, but the universe of polysaccharides is much wider and includes many other polymers that might **also** exhibit potential. **Carrageenan is one of the examples, having a limited number of reported applications in drug delivery. It is extracted from red seaweed and is composed of galactose and 3,6-anhydrogalactose units, linked by alternating α -(1,3) and β -(1,4) glycosidic bonds** (Malafaya et al., 2007; Rinaudo, 2008). Our group has previously reported its use as nanoparticle forming material for drug delivery applications (Grenha et al., 2010b; Rodrigues et al., 2012b). Another of those molecules is pullulan, a neutral polymer consisting of α -(1,6)-linked maltotriose residues, which in turn are composed of three glucose molecules connected to each other by an α -(1,4) glycosidic bond (Chiellini et al., 2008; Mizrahy and Peer, 2012; Namazi et al., 2011). Pullulan is produced from starch by the fungus *Aureobasidium pullulans* **and evidences water solubility** (Leathers, 2003; Rekha and Chandra, 2007). **Interestingly, it is believed to have a role on the adhesion of the referred fungus to biological surfaces, such as leafs** (Pouliot et al., 2005), which might **unveil bioadhesive properties that are relevant for mucosal/transmucosal applications.**

Moreover, it is expected to be biodegradable, being exposed to the hydrolysis of glycoside bonds and the subsequent metabolism of glucose (Teramoto and Shibata, 2006). Pullulan has been described for the production of drug and gene nanocarriers (Cheng et al., 2011; Gupta and Gupta, 2004b; Jeong et al., 1999; Nochi et al., 2010; Rekha and Chandra, 2007; Shimizu et al., 2008), mainly using hydrophobic derivatives. Pullulan-based nanoparticles were reported to adhere to the nasal epithelium in a study regarding nasal vaccination, demonstrating to exhibit a very important property regarding mucosal administration (Nochi et al., 2010), reinforcing the potential for bioadhesion,

Many polysaccharides might assemble into nanoparticles by a simple and mild method of polyelectrolyte complexation, simply taking benefit from the electrostatic interaction potentiated by opposite charges (Grenha, 2012). The use of organic solvents and other potentially aggressive preparation conditions is thus avoided, not compromising the stability of encapsulated molecules during nanoparticle preparation (Agnihotri et al., 2004; Janes et al., 2001) and, possibly, contributing to increased biocompatibility.

Using neutral polysaccharides like pullulan demands synthesizing charged chemical derivatives that enable using the referred methodology to produce nanoparticles.

In this study, we aimed at exploring the potential of pullulan to produce protein nanocarriers adequate for nasal and lung transmucosal delivery (e.g.), using a mild polyelectrolyte complexation technique. Both positively and negatively charged pullulan derivatives were synthesized and complexed with carrageenan and chitosan, respectively, to produce the nanocarriers. To succeed on the approach, the nanoparticles should efficiently associate proteins such as the model bovine serum albumin (BSA), evidence adequate size (up to 500 nm) and positive zeta potential, and be devoid of cell toxicity.

2. Experimental

2.1. Chemicals

Chitosan (CS, low molecular weight, deacetylation degree = 75-85%), glacial acetic acid, phosphotungstic acid, glycerol, BSA, phosphate buffered saline (PBS) tablets pH 7.4, glucose, sucrose, lactose, trehalose, thiazolyl blue tetrazolium bromide (MTT), dimethyl sulfoxide (DMSO), dialysis tubing benzoylated 32 mm (1.27 in), Dulbecco's Modified Eagle's Medium (DMEM), non-essential amino acids (100%), L-glutamine 200 mM, penicillin-streptomycin solution, trypsin-EDTA solution and trypan blue solution (0.4%) were supplied by Sigma Chemicals (Germany). Pullulan was kindly provided by Hayashibara (Japan). κ -Carrageenan (CRG) and potassium bromide (KBr) were obtained from FMC Biopolymer (Norway) and Riedel-del-Haën (Germany), respectively. Foetal bovine serum (FBS) was supplied by Invitrogen (USA). Acetonitrile (HPLC grade) was purchased from JT Baker (Netherlands) and trifluoroacetic acid (TFA) from Alfa Aesar (Germany). Ultrapure water (Mili-Q Plus, Milipore Iberica, Spain) was used throughout. All other reagents were chemical grade. Prior to use, acetonitrile and 0.1% TFA aqueous solution prepared with ultrapure water were filtered with a 0.2 μ m filter.

2.2. Cell line

The Calu-3 cell line was obtained from the American Type Culture Collection (Rockville, USA) and cells were used between passages 37-50. Cells were grown using 75 cm² flasks in a humidified 5% CO₂/95% atmospheric air incubator at 37 °C. The used cell culture medium was 500 ml DMEM, supplemented with 10% foetal bovine serum (FBS), 1% non-essential amino acid solution, 1% L-glutamine and 1%

penicillin–streptomycin. Medium was exchanged every 2-3 days and cells were subcultured weekly.

2.3. Synthesis of pullulan derivatives

Pullulan was chemically modified in order to obtain two derivatives with opposite charge. The negatively charged derivative (**sulfated pullulan, SP**) was obtained through **sulfation** of pullulan, while the positively charged derivative (**aminated derivative, AP**) was synthesised by amination of the original polymer. Both synthesis were performed according to previously described **methodologies** (Simkovic et al., 2009; Yuan et al., 2005) and are specifically described elsewhere (Dionísio et al., 2011). For the preparation of the aminated pullulan, the alkylating agent (glycidyltrimethylammonium chloride; 9 eq) was added to a solution of the polymer in aqueous potassium hydroxide (0.1 g/ml of the polymer and 9 eq of the base) and the resulting mixture heated at 60 °C for 24h. The solution was then neutralised by the addition of HCl (2M). In the preparation of the sulfate derivative, the sulfation agent (SO₃•DMF complex) was first obtained by dropping 20 ml of HClSO₃ into 100 ml of cooled DMF. Pullulan was dispersed in DMF at approximately 0.025 g/mL by heating at 60 °C for 30 min and then the SO₃•DMF complex (9 eq) was added and the mixture allowed to react at the above temperature for 4 h. The mixture was then allowed to cool down and was neutralized with 30% NaOH solution. Both modified polymers were purified by dialysis, recovered by precipitation from ethanol, separated from the supernatant by centrifugation and dried under vacuum.

2.4. Preparation of pullulan-based nanoparticles

Different formulations of nanoparticles were prepared by polyelectrolyte complexation, combining **SP with CS** and **AP with CRG**, thus obtaining SP/CS and CRG/AP

nanoparticles. To do so, CS was dissolved in 1% (w/w) acetic acid to obtain a solution of 1.0 mg/ml (pH 3.2), SP and AP were dissolved in purified water to obtain stock solutions of 1.0 mg/ml (pH 4.5 and 5.7, respectively) and CRG was dissolved in water, resulting in a stock solution of 2.5 mg/ml (pH 6.7).

All nanoparticle formulations were produced by dropping 1 ml of the solution containing the polymer present in the lower amount (negatively charged polymer) over 1 ml of the polymer present in higher amount (positively charged polymer), under mild magnetic stirring (approximately 10 min), at room temperature. CS and AP assumed a fixed concentration of 1 mg/ml in the formulations SP/CS and CRG/AP, respectively, and the other stock solutions were appropriately diluted to obtain nanoparticles of SP/CS and CRG/AP mass ratios of 1/2, 1/3 and 1/4 (w/w). The pH of nanoparticle suspensions was 3.3 and 5.9 for SP/CS and CRG/AP, respectively. Nanoparticles were then isolated by centrifugation at $16,000 \times g$ on a 10 μ l glycerol layer for 30 min at 15 °C (Eppendorf 5804R, Eppendorf, Germany). The supernatants were discarded and nanoparticles were resuspended in 200 μ l of purified water.

BSA was chosen as a model protein and was incorporated in the formulations (SP/CS = 1/2 and CRG/AP = 1/2) in a theoretical content of 30% (w/w) respective to the polymer present at the higher concentration (CS or AP). To prepare protein-loaded nanoparticles, BSA was dissolved in water and mixed with the solution corresponding to the polymer present in the lower amount prior to dropping over the other polymer for the polyelectrolyte complexation to take place (the pH of SP/BSA mixture is 5.1 and that of CRG/BSA mixture is 6.5). The final pH of BSA-loaded nanoparticles was the same observed for the unloaded nanoparticles.

2.5. Characterisation of nanoparticles

The morphological examination of nanoparticles was conducted by transmission electron microscopy (TEM) (JEM- 1011, JEOL, Japan). Samples were stained with 2% (w/v) phosphotungstic acid and placed on copper grids with carbon films (Ted Pella, USA) for TEM observation. Measurements of nanoparticle size and zeta potential were performed on freshly prepared samples by photon correlation spectroscopy and laser Doppler anemometry, respectively, using a Zetasizer Nano ZS (Malvern Instruments, Malvern, UK). For the analysis of particle size and determination of the electrophoretic mobility, each sample was diluted to the appropriate concentration with ultrapure water and placed in the electrophoretic cell ($n \geq 3$).

2.6. Determination of nanoparticle production yield

The yield of nanoparticle production was calculated by gravimetry. Fixed volumes of nanoparticle suspensions were centrifuged ($16,000 \times g$, 30 min, 15 °C), and sediments were freeze-dried using a Labconco freeze dryer (Labconco, USA) ($n = 6$).

The production yield (PY) was calculated as follows:

$$PY = (\text{Nanoparticle sediment weight} / \text{Total solids weight}) \times 100 \quad (\text{Eq. 1})$$

where nanoparticle sediment weight is the weight after freeze-drying and total solids weight is the total amount of solids added for nanoparticle formation.

2.7. Nanoparticle analysis by Fourier transform infrared (FTIR) spectroscopy

The presence of the different components of the nanoparticulate systems was verified by FTIR. Infrared spectra of the specimen powders, namely CS, CRG, AP and SP, as well as of the two formulations of nanoparticles ($SP/CS = 1/2$ and $CRG/AP = 1/2$), were recorded using a FTIR spectrophotometer (Tensor 27, Bruker, Germany). BSA-loaded

nanoparticles were assessed in the same conditions, and BSA was also analysed as control.

Nanoparticles were freeze-dried prior to the assay and all the samples were gently triturated with KBr and compressed into discs for the analysis.

For each spectrum a 32-scan interferogram was collected in transmittance mode with a 4 cm^{-1} resolution in the $4000\text{--}400\text{ cm}^{-1}$ region at room temperature.

2.8. Determination of protein loading capacity of nanoparticles

BSA association efficiency was determined upon separation of nanoparticles from the aqueous preparation medium containing the non-associated protein by centrifugation ($16,000 \times g$, 30 min, $15\text{ }^{\circ}\text{C}$). The amount of free BSA was determined in the supernatant by HPLC (Agilent 1100 series, Germany). The chromatographic conditions used to quantify the protein were: mobile phase consisted of acetonitrile and 0.1% TFA aqueous solution initially set in the ratio 30:70 (v/v), which was linearly changed to 40:60 (v/v) over 5 min. From 5 to 10 min the ratio 40:60 (v/v) was kept constant. Eluent was pumped at a flow rate of 1 ml/min, the injection volume was 20 μl and detection wavelength was 280 nm. A calibration curve of the protein was made in PBS (pH 7.4). All experiments occurred at room temperature and the total area of the peak was used to quantify BSA ($n = 3$).

The protein association efficiency (AE) and the loading capacity (LC) of nanoparticles were calculated as follows:

$$\text{AE (\%)} = [(\text{Total BSA amount} - \text{Free BSA amount}) / \text{Total BSA amount}] \times 100 \quad (\text{Eq. 2})$$

$$\text{LC (\%)} = [(\text{Total BSA amount} - \text{Free BSA amount}) / \text{Nanoparticle weight}] \times 100 \quad (\text{Eq. 3})$$

2.9. *In vitro* release of BSA from nanoparticles

The release of BSA was determined by incubating 1 ml of nanoparticles of each formulation (SP/CS = 1/2 and CRG/AP = 1/2) in 5 ml PBS pH 7.4, under horizontal shaking at 37 °C. At appropriate time intervals (1, 2, 3, 4, 6, 8 and 24h) samples of 100 µl were collected to quantify the amount of protein released by HPLC (Agilent® 1100 series, Germany). Each time a sample was removed, the corresponding volume was replaced with the same amount of PBS (n = 3).

2.10. Study of nanoparticle stability and freeze-drying

Aliquots of nanoparticle formulations (SP/CS = 1/2 and CRG/AP = 1/2) were kept at 4 °C to evaluate nanoparticle stability upon storage. Size and zeta potential were monitored as a function of time for approximately 30 days, using the techniques described above (n = 3).

With the aim of developing a pharmaceutically-acceptable dry form of the nanoparticle suspensions, the same formulations were submitted to a freeze-drying study.

Nanoparticles were concentrated by centrifugation and their concentration was set at 2 mg/ml. Nanoparticle suspensions (1 ml) were freeze-dried in the presence of four carbohydrates (sucrose, glucose, lactose and trehalose), which were used separately as cryoprotectants and tested at different concentrations (2.5, 5 and 10%, w/v). Samples were freeze-dried under the following conditions: pressure of 50-100 Torr, 24h of primary drying starting at -35 °C and gradually increasing until -10 °C, 24h at 0 °C and a final step of secondary drying (12 – 24h) at 15 °C (Labconco Corp., USA). After freeze-drying, the nanoparticles were resuspended by adding the volume of water corresponding to the initial volume (1 ml), and their size and zeta potential were determined as indicated above.

2.11. *In vitro* cytotoxicity study of pullulan-based nanoparticles

The *in vitro* cytotoxicity of pullulan-based nanoparticles, as well as that of the raw materials involved in nanoparticle production, was assessed by the metabolic assay thiazolyl blue tetrazolium bromide (MTT) test. The original unmodified polymer of pullulan was also assessed. Cells were seeded at a density of 2.5×10^4 cells/well in 96 well plates, suspended in 100 μ l of cell culture medium. After 24h at 37 °C in 5% CO₂ atmosphere, the medium was replaced by fresh medium containing the test samples with polymers/nanoparticles or controls. Cells incubated with either 2% (w/v) SDS solution or culture medium were used, respectively, as positive and negative control of cell death. All formulations and controls were prepared in pre-warmed cell culture medium without FBS immediately before application to the cells. Samples were tested for 3h and 24h at different concentrations (0.1, 0.5 and 1.0 mg/ml). After incubation with the test solutions, the medium containing the particles/polymers was removed and 30 μ l of MTT solution (0.5 mg/ml in PBS, pH 7.4) added on each well. After 2h, the medium was removed and the formazan crystals dissolved in 50 μ l of DMSO. The absorbance of each well was measured by spectrophotometry using a plate reader (Teacan-Infinite M200, Switzerland) at 540 nm and corrected for background absorbance using a wavelength of 650 nm.

Cell viability was calculated as follows:

$$\text{Cell viability (\%)} = (A-S)/(CM-S) \quad (\text{Eq. 4})$$

where A is the absorbance obtained for each of the concentrations of the test substance, S is the absorbance obtained for 2% SDS and CM is the absorbance obtained for untreated cells (incubated with cell culture medium). The latter reading was assumed to correspond to 100% cell viability. The assay was performed on three occasions with six replicates at each concentration of test substance in each instance.

2.12. Statistical analysis

For the generality of results, the t-test and the one-way analysis of variance (ANOVA) with the pairwise multiple comparison procedures (Student-Newman-Kleus Method) were performed to compare two or multiple groups, respectively. These analyses were run using the SigmaStat statistical program (Version 3.5, SyStat, USA).

The cytotoxicity assay was performed according to a factorial design (FD), used to investigate the effect of time (X_1), concentration (X_2) and polymers/nanoparticles (X_3) on cell viability (Y). A three-way ANOVA with three independent variables was performed and the levels of two variables were the following: 3h, 24h (X_1) and 0.1, 0.5 and 1 (X_2). The third variable (X_3) has different attributes: 1) when polymers are considered, the levels of X_3 are CS, CRG, pullulan, AP and SP; in the case of nanoparticles, the levels are CRG/AP and SP/CS. For either polymers or nanoparticles, the objective is to investigate the influence of the three factors (X_1 , X_2 and X_3) on the response factor (Y). Further analyses with Post hoc tests were used to determine which groups differ. FD was performed with SPSS (version 21.0 for windows) and the effect plots were obtained with package gplots from R 2.15.3 software (Meyres et al., 2012; R Core Team, 2013).

All the statistical analyses were performed at a level of significance of $\alpha = 5\%$.

3. Results and Discussion

3.1. Preparation and characterisation of nanoparticles

Several formulations of pullulan-based nanoparticles were produced by a mild procedure of polyelectrolyte complexation that involves an electrostatic interaction between oppositely charged polymers. This is a very simple procedure, which most important advantages are the complete hydrophilic environment and the mild

preparation conditions, thus avoiding the use of organic solvents or high shear forces (Grenha, 2012; Prego et al., 2005b). From its characteristics, pullulan holds potential for the preparation of nanocarriers. However, it is a neutral polymer and, therefore, cannot be used directly to obtain nanoparticles by this methodology. To overcome this limitation, a positively charged amine derivative (137 kDa) and a negatively charged sulfated derivative (10 kDa) of pullulan were synthesised (Dionísio et al., 2011). Based on the estimations performed from elemental analysis data, the sulfation reaction resulted in approximately 4 sulfate groups per maltotriose unit (SP), while a degree of substitution of approximately 3 amino groups per repeating unit was found for AP. The former was assumed to be in the sodium salt form, to which corresponds a mass of 904 g/mol and, the latter, to be in the form of chloride salt, with a mass of 885 g/mol (unpublished results). For CS, a mean value of 0.8 positive charges per monomer, and an average monomeric molecular weight of 169 g/mol were used. Carrageenan was assumed to be in the sodium salt form, to which corresponds a mass of 408 g/mol and a negative charge per disaccharide monomer unit (Rodrigues et al., 2012b).

The chemical structures of pullulan derivatives, as well as those of the other polymers involved in the production of nanoparticles are depicted in **Figure 1A**.

Unloaded SP/CS and CRG/AP nanoparticles of mass ratios 1/2, 1/3 and 1/4 were prepared, the former displaying sizes around 250 nm and the latter around 180 nm, and all showing high positive zeta potential. For both polymeric compositions, minimal changes on size and zeta potential were observed due to mass ratio modification (data not shown). For both formulations SP/CS and CRG/AP, the mass ratio of 1/2 displayed higher production yield, which is easily justified by the proper mechanism of nanoparticle formation due to electrostatic interaction. CS and AP were used at a fixed concentration of 1 mg/ml in each formulation and the second polymer was added in

variable concentrations (the amount decreasing from 1/2 to 1/4) to obtain the different mass ratios. Therefore, as the formulations with mass ratio 1/2 are those integrating the higher amount of negative polymer, a higher degree of interaction between negatively and positively charged groups is potentiated, leading to the formation of a higher number of nanoparticles (Fernández-Urrusuno et al., 1999b; Grenha et al., 2005; Rodrigues et al., 2012b). In fact, in SP/CS formulations, positive to negative (+/-) charge ratios vary from 2 to 4, and in CRG/AP formulations, from 3 to 6, as the amount of negatively charged polymer decreases. Therefore, mass ratios of 1/2 approach the most the stoichiometric amount of charges.

Taking this into account, the formulations SP/CS and CRG/AP of mass ratio 1/2 were selected to perform further studies. As can be observed in **Figure 2**, pullulan-based nanoparticles evidence similar structure and morphology, corresponding to spherical and compact nanoparticles. This morphology corresponds to that widely reported for many formulations of polysaccharide-based nanoparticles (Calvo et al., 1997b; Goycoolea et al., 2009; Oyarzun-Ampuero et al., 2009; Sarmiento et al., 2006; Teijeiro-Osorio et al., 2009; [Zorzi et al., 2011](#)).

The physicochemical properties of these nanoparticles are displayed in **Table 1**. SP/CS nanoparticles display a size of 260 nm and a strong positive zeta potential of +50 mV. CRG/AP nanoparticles have a lower size of approximately 185 nm ($P < 0.05$) and a similar zeta potential of +56 mV. The positive zeta potential results from the higher amount of the positively charged polymer in both cases. The polydispersion index is in all cases between 0.2 and 0.4 and production yields are similar for both [formulations \(around 55 – 60%\)](#).

The difference registered for the nanoparticle size might result from different intensity of electrostatic interactions due to the use of polymers with different charge [densities](#).

Lower charge ratios thus lead to the formation of larger nanoparticles, as happens for the SP/CS formulation, because there is a higher amount of negative charges to neutralise the positive groups, reducing electrostatic repulsion. Actually, although not to a significant level, the zeta potential of SP/CS nanoparticles is lower than that of AP/CRG nanoparticles, possibly reflecting the higher amount of negative charges present in the former formulation. This effect of size decrease with the increase of +/- charge ratio was previously reported in another work from our group, involving the preparation of chitosan/carrageenan nanoparticles (Rodrigues et al., 2012b).

The presence of the different components on the nanoparticulate systems was assessed by FTIR. The obtained spectra are displayed in **Figure 1B-C**. The presence of SP in SP/CS nanoparticles is apparent in the respective spectrum by a S=O asymmetric stretching band at 1254 cm^{-1} ; although the CS amide bands are partially masked by the band of adsorbed water bending at approximately 1640 cm^{-1} (Wilson et al., 2000), its presence is denoted by the new band at 1541 cm^{-1} due to absorption of the protonated amino groups. Since the quaternary ammonium groups do not display characteristic IR absorption bands (Nakanishi et al., 1957), evidence for its presence in the AP/CRG nanoparticles comes from the bands at 1477 and 926 cm^{-1} (C-H scissoring in methyl groups of the ammonium and ether C-O asymmetric stretching, respectively) (Xu et al., 2003); CRG presence is denoted by the sulfate band at 1261 cm^{-1} .

BSA was selected as model to test the ability of pullulan-based nanoparticles to associate proteins. The FTIR spectra of BSA-loaded nanoparticles evidence the effective association of protein to the nanoparticle structure. The spectra of loaded particles match those of the blank counterparts, evidencing incorporation of the two polymers in both formulations. In the case of SP/CS nanoparticles, the presence of the protein enhanced the intensity of the 1645 and 1541 cm^{-1} bands, due to superposition

with the amide I and amide II bands, respectively; the former was also shifted to a higher wavenumber. Also, the band at 1258 cm^{-1} is stronger in the loaded particles, due to superposition of the 1254 cm^{-1} band of sulphate and the amide III band, at 1247 cm^{-1} . In the CRG/AP loaded particles, the presence of the protein is denoted by an intensity enhancement and shift to a higher wavenumber of the 1647 cm^{-1} band, the appearance of a new band at 1558 cm^{-1} , and the broadening of the band at 1256 cm^{-1} , for the aforementioned reasons.

It is widely accepted that the interactions between proteins and polyelectrolytes are predominantly of electrostatic nature (Cooper et al., 2005). In fact, BSA presents both basic and acidic groups on its surface, in a fairly uniform distribution, providing the protein with an amphiphilic character. Due to that surface charge anisotropy, BSA presents positive and negative charge domains (“patches”), the latter more dispersed. Such characteristics allow BSA to bind polyanions at $\text{pH} > \text{pI}$, where the protein presents a global negative charge, forming soluble complexes. This binding “on the wrong side” of the pI was ascribed to an interaction of the polyanion with the positive domain of the protein, thus resulting in a combination of short-range attractive interactions coupled with longer-range repulsive interactions. Lowering the pH below pI leads to coacervation, due to charge neutralization of the polyanion by the globally positive protein (Seyrek et al., 2003). On the contrary, binding of BSA to polycations “on the wrong side” of the pI is not favored because its negative domains are fragmented, thus being ineffective at binding polycations, with the long-range repulsion prevailing over the short-range attraction. Only at pH above pI , where wider negative domains form, soluble complexes are observed, with coacervation occurring at even higher pH values (Chen et al., 2011).

As referred in section 2.4, BSA is mixed with either SP or CRG (the negatively charged polymers) prior to the addition to CS or AP solutions, respectively. The first mixture has, in both cases, a pH above BSA isoelectric point (4.7) and, therefore, BSA presents a negative charge. Under such circumstances, the formation of soluble complexes, with a global negative charge, between the protein and the polysaccharides is expected, thus potentiating the electrostatic interaction with the positively charged polymers and protein encapsulation.

In this study, the physicochemical characteristics of nanoparticles generally remained unaltered after protein association, with the exception of a slight increase in AP/CRG nanoparticles size from 185 to 244 nm ($P < 0.05$). Although the general little or absent effect on physicochemical properties (size and/or zeta potential) upon BSA association is somewhat unexpected, it has been registered in several studies on nanoparticles obtained by polyelectrolyte complexation (de la Fuente et al., 2008b; Grenha et al., 2007; Liu et al., 2007; Vandana and Sahoo, 2009). BSA association with macromolecules has been reported not to be uniform as, to a certain extent, the pattern of association is governed by the 3D conformation that the protein adopts at specific pH and ionic strength. The protein has both positive and negatively charged functional groups, but it also has hydrophobic regions that tend to fold in a 3D structure in aqueous environment (Yampolskaya and Platikanov, 2006). In turn, polymeric molecules might adopt a spread conformation in solution because of electrostatic repulsion between charged groups along the molecular chain. The carboxyl groups on the surface of a large protein like BSA may bind to positively charged groups at certain sites of the spread polymeric chain of either CS or AP, but still maintaining a compact structure of the protein itself, so as to keep an inner hydrophobic core. Therefore, it is possible to assume that protein association does not neutralise significantly the positive surface

charge of chitosan or aminated pullulan molecules (Gan and Wang, 2007). Also, although there is the possibility of further protein adsorption on the surface of formed nanoparticles, this would occur by interaction of the negative domains of the former, with the positive charge of the latter, therefore partially or totally neutralizing the protein negative global charge (Chen et al., 2011). Moreover, in the case of SP/CS nanoparticles, the final solution pH is 3.3, well below BSA *pI*. In this manner, eventual protein adsorption on the particles surface is not expected to enormously affect their surface potential, as was observed.

Production yield remained between 20 and 30%, even after association of the protein. BSA was associated with efficiencies of approximately 35-45% for CRG/AP and SP/CS nanoparticles, achieving loadings around 30%. Comparisons established at this level with other works are possibly not very useful, as they will concern nanoparticles produced with different materials and even different proteins. Nevertheless, regarding the loading capacity, nanoparticles presented in this study evidence similar ability as that of other formulations of polysaccharide-based nanoparticles (Chen et al., 2008; Fernández-Urrusuno et al., 1999a; Grenha et al., 2007; Oyarzun-Ampuero et al., 2009).

3.2. *In vitro* release of BSA from nanoparticles

Figure 3 shows the *in vitro* release of BSA in PBS pH 7.4, a medium that intends to resemble the environment of mucosal surfaces like the pulmonary (Walters, 2002), although in some cases it has also been used in the context of nasal delivery (Amidi et al., 2006; Amidi et al., 2007; Fernández-Urrusuno et al., 1999a). Results indicate that, for both formulations, the release of BSA from nanoparticles shows an initial burst, releasing approximately 30% of the encapsulated protein in 2h. However, at that time a steady state is achieved and no further release is observed up to 24h. This initial burst

release might correspond to the amount of protein that is located at the surface of the nanoparticles, which thus easily desorbs, an effect that has been reported in other studies (Amidi et al., 2006). Other works available in the literature describe quite similar release behaviour. *N*-trimethylchitosan nanoparticles designed for nasal delivery also released rapidly (3h) 30% of the associated protein in the same medium, although the assay was not prolonged beyond that (Amidi et al., 2006). In chitosan/tripolyphosphate nanoparticles it has been seen that BSA releases very slowly, for several days (Calvo et al., 1997a, b; Gan and Wang, 2007). However, in one of the mentioned works, at 48h the amount of release is around 30%, although no measurement was taken before this time (Calvo et al., 1997a), while in the other a release of approximately 30% was obtained in 24h (Gan and Wang, 2007).

The relevance of this release profile is intimately dependent on the contextualisation with an administration route. If the approach of transmucosal lung delivery is considered, for instance, as exemplified above to justify the used release medium (pH 7.4), it is generally accepted that particles remain in the lung for up to 24h, although those deposited in the alveolar zone might expect prolonged retention time because of the absence of mucociliary clearance (Hofmann and Asgharian, 2003; Möller et al., 2006). In turn, if nasal administration is focused, for instance, the frequent turnover of nasal mucus will strongly decrease the retention time (Illum, 2002; Lansley and Martin, 2001) and, even if mucoadhesive formulations are applied, shorter contact time is expected as compared with lung delivery. Nevertheless, if nasal delivery is focused, a pH that resembles more closely the environment of the nasal cavity (5.5 – 6.5) (Lansley and Martin, 2001) should be used for the release studies.

3.3. Nanoparticle stability in storage and upon freeze-drying

One of the problems of colloidal drug carriers is their low stability and tendency to aggregate, which is known to be affected by many factors, with both physical (aggregation/particle fusion) and chemical instability (hydrolysis of polymer and chemical reactivity) appearing along time when nanocarriers are formulated as aqueous suspensions (Abdelwahed et al., 2006; Chacon et al., 1999; Kumar et al., 2012). The natural tendency for aggregation upon storage is actually one of the important limitations of nanoparticle application (Sameti et al., 2003; Wu et al., 2011). This tendency is attributed to the fact that, when two particles come into contact, the attractive potential is much greater than the kinetic energy that could induce their separation (Ikeda and Zhong, 2012). In this regard, the use of charged nanoparticles, as those described in this work, might prevent aggregation and has been proposed as strategy to increase nanoparticle stability.

In order to study nanoparticle behaviour in storage, the size and zeta potential of SP/CS and CRG/AP nanoparticles were monitored along time. It was observed that, for up to approximately 1 month, both formulations maintain reasonably the initial physicochemical characteristics when stored at 4 °C (data not shown). There is a significant ($P < 0.05$), although slight, decrease in the zeta potential of CRG/AP nanoparticles at the beginning of the assay from +65 mV to +56 mV, but this did not induce any effect on nanoparticle size, as the zeta potential remains sufficiently high to induce repulsion of nanoparticles. Chitosan-based nanoparticles have been reported to exhibit physicochemical stability in similar time intervals (Hafner et al., 2009; Morris et al., 2011; Rodrigues et al., 2012b). No similar studies are reported for pullulan-based nanoparticles, thus not allowing a direct comparison.

Although pullulan-based nanoparticles demonstrated to remain stable at 4 °C for at least one month, it was decided to develop lyophilized formulations that provide stability for longer periods of time. The optimal conditions for freeze-drying were studied, testing glucose, sucrose, trehalose and lactose as cryoprotectants. Formulations elaborated with both pullulan derivatives evidenced a general maintenance of zeta potential values (data not shown), as the ratio “after freeze-drying/ before freeze-drying” varied between 1 and 1.2.

Figure 4 displays the variation of nanoparticle size when comparing that obtained after reconstitution of freeze-dried material (Df) with the initially determined (Di) before the freeze-drying process. The direct freeze-drying of nanoparticles (without cryoprotectants) did not preserve their properties (data not shown), leading to strong aggregation. This is justified by the high concentration of particles occurring during the freezing step and to the mechanical stress induced by ice crystallisation (Abdelwahed et al., 2006; Vauthier and Bouchemal, 2009). The two formulations of nanoparticles behaved differently in the presence of the tested cryoprotectants. CRG/AP nanoparticles (**Figure 4A**) were more difficult to stabilise than SP/CS nanoparticles (**Figure 4B**). In the former, glucose at a concentration of 5% or higher provided the best conditions for nanoparticle stabilisation during the freeze-drying process ($P < 0.05$), although a slight increase in the nanoparticle size was still observed (from 204 nm to 249 nm). Sucrose and trehalose had only a small cryoprotectant effect, as nanoparticle size was increased considerably ($p < 0.05$) after freeze-drying, doubling in several cases. Finally, lactose (a typical excipient used in lung delivery) revealed absolutely inefficient as cryoprotectant agent, permitting strong aggregation after freeze-drying. This negative performance of lactose was previously reported, being attributed to its poor protective effect during the freezing step (Hirsjärvi et al., 2009). Notwithstanding the apparent ability of glucose for

the physicochemical stabilisation of CRG/AP nanoparticles, this excipient should be used cautiously, as it has been referred as not adequate for protein formulations, because of its reducing character (Li et al., 1996; Wang, 2000). Nevertheless, the freeze-drying of protein nanocarriers in presence of glucose has been reported as efficient, not only regarding the physicochemical stability of the carrier, but also considering the maintenance of protein properties (Freixeiro et al., 2013). In any case, a comprehensive review on the subject suggests that it should be evaluated on a case-by-case basis (Wang, 2000).

SP/CS nanoparticles demonstrated an easier stabilisation. Again, lactose demonstrated to be ineffective as cryoprotectant, although the obtained sizes were much lower as compared to those of CRG/AP nanoparticles when stabilised by the disaccharide.

Sucrose, glucose and trehalose presented in this case a comparable behaviour, generally maintaining the stability of nanoparticles, even at the lower concentration of 2.5%. A concentration of 10% sucrose or glucose resulted in a mean size slightly lower than that observed before freeze-drying. This effect was observed in other studies, evidencing a compaction of nanoparticle structure during the freeze-drying process (de la Fuente et al., 2008b).

It is noteworthy that both formulations of nanoparticles responded differently to the presence of the tested cryoprotectants. CRG/AP nanoparticles evidenced a D_f/D_i ratio between 1 and 3, which was many times close to or above 2, demanding higher cryoprotectant concentrations to achieve a stabilising effect. On the contrary, the D_f/D_i ratio observed for SP/CS nanoparticles varied between 1 and 2 and in most cases remained close to 1, indicating that lower cryoprotectant concentrations were sufficient for the stabilisation of nanoparticles. These differences are possibly related with the composition of nanoparticles. Different chemical groups are exposed to the outer

surface in each formulation and, consequently, the interaction mediated with the cryoprotectant is different (Abdelwahed et al., 2006), an effect that is known to greatly affect the cryoprotective effect.

Although the obtained results suggest that the conditions to stabilise both formulations of nanoparticles were found, a relevant subsequent step is testing the stability of protein-loaded nanoparticles, as it is known that the entrapped drug may influence the freeze-drying of nanoparticles (Abdelwahed et al., 2006). Additionally, and particularly in the case of CRG/AP nanoparticles, the stabilisation conditions can be improved to avoid the slight size increase that is still observed when glucose is used as cryoprotectant. The studies should also be further completed to verify whether freeze-drying affects the release pattern and the biological activity of the encapsulated protein.

3.4. *In vitro* cytotoxicity study of pullulan-based nanoparticles

Addressing the biocompatibility of drug carriers is a major issue in developing drug delivery systems (Gaspar and Duncan, 2009; Liu et al., 2008; Rodrigues et al., 2012a) and current international guidelines require the contextualisation of biocompatibility with a specific route of administration and dose of the material (Gaspar and Duncan, 2009). In turn, it is also mandatory to treat polymers and polymer-based carriers as different entities, as the proper carrier structure, among other parameters, might affect the final behaviour (Aillon et al., 2009; Gaspar and Duncan, 2009; Williams, 2008). According to the guidelines issued by the International Organisation for Standardisation (ISO), testing biocompatibility implies the performance of a complete set of assays, addressing at first cellular morphology, membrane integrity and metabolic efficiency, but in some cases also including genotoxicity, as well as acute and sub-acute toxicity (ISO, 2003, 2009a, b; Rodrigues et al., 2012a). In this work we performed one of the

most used assays to test the cytotoxicity of materials and carriers, which is the metabolic assay MTT. This assay assesses cells metabolic efficiency, relying on the evaluation of enzymatic function. To do so, after the exposure to the test materials/carriers, cells are incubated with yellow tetrazolium (MTT) salts which are reduced to purple-blue formazan crystals by active mitochondrial dehydrogenases (Rodrigues et al., 2012a). In this manner, a higher concentration of the formazan dye corresponds to a higher amount of metabolically active cells, which is usually interpreted as higher cell viability.

The Calu-3 is an immortalised cell line obtained from lung adenocarcinoma and has been extensively used in the study of formulations designed for either nasal or pulmonary drug administration, as it is considered a model of the epithelium of both regions (Casettari et al., 2010; Grainger et al., 2006; Zhu et al., 2010). Importantly, the MTT assay has been referenced as an effective tool to evaluate and compare the toxicity of materials on respiratory cells, namely the Calu-3 (Scherließ, 2011).

The MTT assay was performed according to a factorial design consisting of either twelve (nanoparticles) or thirty (polymers) factor/level combinations. **Figure 5** depicts the general statistic outcome, evidencing the variables and combinations that have an effect on cell viability (Y). Concerning the polymers (**Figure 5A**), the type of polymer (X_3) and the used concentration (X_2) were found to have the most relevant effect on cell viability, followed by the combinations time/type of polymer ($X_1 * X_3$), concentration/type of polymer ($X_2 * X_3$) and the three-way interaction ($X_1 * X_2 * X_3$) ($P < 0.05$). Obtaining a statistically significant effect indicates that the means of the groups are significantly different. However, it does not inform on which pairs of means the significant differences refer to. To do so, the analysis should include testing the various levels of the variables. Testing the levels of X_1 (3h and 24h) with other variables

revealed statistical differences ($P < 0.05$) for some polymers (CS, CRG, AP). Nevertheless, as can be observed in **Figure 6**, the differences are generally devoid of biological relevance, as cell viability remains around 80-100%, which is considered very acceptable. Noticeably, at 3h (**Figure 6A**) aminated pullulan induces cell viabilities between 70% and 45%. For this pullulan derivative, there is a concentration dependent behaviour, as the cytotoxic effect is much more pronounced for 0.5 and 1.0 mg/ml (50-45% cell viability) than for 0.1 mg/ml (69% cell viability) ($P < 0.05$). Upon 24h exposure (**Figure 6B**), all polymers resulted in cell viability above 80%, with the exception of aminated pullulan. The latter registered the highest toxicity ($P < 0.05$), decreasing cell viability to 42-49%, independently of the concentration. Aminated pullulan is thus observed to have a clear time-dependent effect ($P < 0.05$), evidencing the most differentiating behaviour, corresponding to a cytotoxic effect.

The influence of surface charges on cytotoxicity remains largely unresolved, but there are many indications suggesting a role of this parameter on cellular uptake and on the cytotoxicity of substances. In this context, positively charged materials have been frequently found to be more cytotoxic than neutral or negatively charged counterparts, because positive charges provide a means for stronger interaction with cell surfaces, in many cases associated with internalisation of the material (Bhattacharjee et al., 2010; Ilinskaya et al., 2002; Turcotte et al., 2009). Curiously, in this case, although chitosan is also positively charged, it does not evidence any cytotoxic effect, cell viability remaining around 100% irrespective of the used dose or time of exposure to the polymer solution. Two possible justifications for that effect could be a different charge density and a different size of the polymer chains. Regarding the latter parameter, an interesting work on the subject evaluated the cytotoxic effect of cationic pullulan microparticles on human leukemic K562(S) cells, demonstrating that increased molar

concentration of amino groups induced higher cytotoxicity (Constantin et al., 2003). Chitosan and aminated pullulan have approximately the same number of positive charges (0.8/chitosan monomer and 1/aminated pullulan monomer), thus not constituting a possible explanation for such a different behaviour. In parallel, the polymers present similar molecular weight. The main reason for the different behaviour should be instead the fact that amino groups of chitosan tend to deprotonate above the pK_a of the polymer (approximately 6.4) while pullulan remains positively charged at pH 7.4, which is approximately that of the nanoparticle suspension in cell culture medium. Although not directly used in the production of the nanoparticles presented in this work, unmodified pullulan was also tested, because its application in drug delivery has been reported, but data on its effect on epithelial cells are not available on the literature. As can be observed, its effect was found to not depend neither on concentration nor on time, resulting in approximately 75-85% cell viability in all cases. This is consistent with results reporting the application of pullulan coating to reduce the cytotoxicity of superparamagnetic iron oxide nanoparticles when in contact with human fibroblasts (hTERT-BJ1 cells) (Gupta and Gupta, 2005) or the same effect when coating magnetite nanoparticles (L929 fibroblasts) (Gao et al., 2010). As such, the coupling of cholesterol-modified pullulan nanoparticles to amyloid- β oligomers was found to reduce the cytotoxicity associated with the oligomers (Boridy et al., 2009), which are thought to have a role on Alzheimer's disease (Sakono and Zako, 2010).

The most prominent result of the cytotoxicity study performed in this work is the fact that, notwithstanding the cytotoxic effect of some raw materials composing the nanocarriers, the exposure to the nanoparticle formulations for 3h or 24h results in cell viabilities between 74% and 94% (Figure 7). These values reveal that, independently of the formulation, concentration or time of incubation, the developed nanoparticles elicit

biologically acceptable cell viabilities. Nevertheless, the statistical analysis of results revealed that some variables had a stronger effect on cell viability as compared with others. As can be observed in Figure 5B, a significant effect on cell viability was found for concentration (X_2), for the interaction between time of incubation and nanoparticle formulations (X_1*X_3), and also for the three-way interaction ($X_1*X_2*X_3$) ($P < 0.05$). The effect plot suggests that the concentration has one of the most important effects on cell viability and, therefore, the three levels of concentration (0.1, 0.5 and 1.0 mg/ml) were compared. The results generally indicate that the lower concentrations (0.1 and 0.5 mg/ml) have a similar contribution to cell viability, as a concentration increase at this level does not have a significant effect. In turn, when nanoparticle concentration is increased to 1 mg/ml, cell viability tends to decrease significantly ($P < 0.05$).

Additionally, the analysis of simple effects was performed regarding the three-way interaction term. It was found that, for 3h incubation with CRG/AP nanoparticles, an increase in concentration from 0.5 to 1 mg/ml induced a decrease in cell viability from 87% to 74% ($P < 0.05$). At 24h, cell viability remained constant around 88%. For SP/CS nanoparticles, an effect of concentration was only observed at 24h, as the viability decreased from 92% (0.1 mg/ml) to 78% when concentration increased to 1 mg/ml. It was found that both formulations presented a different response to the higher concentration of nanoparticles (1 mg/ml) both at 3h and 24h of incubation. Curiously, while SP/CS nanoparticles induced a viability decrease from 90% to 79% ($P < 0.05$) by prolonging the contact time, the opposite was observed for CRG/AP nanoparticles, as cell viability increased from 75% to 89% ($P < 0.05$). Although no plausible justification could be found for that event, it was considered that it does not compromise the general trend of results.

It is important to highlight that the above mentioned tendency of higher toxicity of positively charged materials has been reported many times regarding nanoparticles (Zobel et al., 1999). Nevertheless, this has not been the case for the nanoparticles produced and assessed in this work, although they exhibit a highly positive surface charge.

To our knowledge, the assessment of the cytotoxic effect of pullulan-based nanoparticles on epithelial cells, either Calu-3 or other cell line, has never been reported, thus hindering a valuable and effective comparison. Nevertheless, although performed at different conditions, several works report the absence of a cytotoxic effect of pullulan nanoparticles on various types of cells, like human fibroblasts h-TERT BJ1 (Gupta and Gupta, 2004a), monkey fibroblasts COS-7, human embryonic kidney cells HEK 293 (Gupta and Gupta, 2004b) and mouse macrophage-like cells RAW264.7 (Lee et al., 2012).

As a general trend, it is thus considered that the contact of pullulan-based nanoparticles with the epithelial cells representative of nasal and lung mucosa, does not have an overt effect on cell metabolic activity, thus not compromising normal metabolic functions that are essential for surviving.

4. Conclusions

In this work, aminated and sulfated derivatives of pullulan demonstrated to have the ability to easily assemble into nanoparticles upon polyelectrolyte complexation with either carrageenan or chitosan. The produced nanoparticles displayed size around 200 nm and the strongly positive zeta potential (approximately + 50 mV). Storing the nanoparticle suspensions at 4 °C preserved their physicochemical characteristics (size and zeta potential) for up to one month, while freeze-drying in presence of a

cryoprotectant like glucose also provided stability. The capacity of the nanocarriers to associate a model protein (BSA) was satisfactory and there is great evidence of absence of overt toxicity of the pullulan-based nano delivery systems on a respiratory cell line (Calu-3). Based on these results, and taking into account the reported bioadhesiveness of pullulan, pullulan-based nanoparticles are believed to hold potential for an application in transmucosal protein delivery, with a particular focus on the nasal and pulmonary routes.

Acknowledgements

This work was supported by national Portuguese funding through FCT - Fundação para a Ciência e a Tecnologia, project ref. PTDC/SAU-FCF/100291/2008 and PEst-OE/EQB/LA0023/2011, as well as from the Spanish Government (ISCIII, Acción Estratégica de Salud, PS09/00816). Research of Clara Cordeiro is supported by FCT-PEst-OE/MAT/UI0006/2011.

References

- Abdelwahed, W., Degobert, G., Stainmesse, S., Fessi, H., 2006. Freeze-drying of nanoparticles: Formulation, process and storage considerations. *Advanced Drug Delivery Reviews* 58, 1688-1713.
- Agnihotri, S.A., Mallikarjuna, N., Aminabhavi, T., 2004. Recent advances on chitosan-based micro- and nanoparticles in drug delivery. *Journal of Controlled Release* 100, 5-28.

Aillon, K.L., Xie, Y., El-Gendy, N., Berkland, C.J., Forrest, M.L., 2009. Effects of nanomaterial physicochemical properties on in vivo toxicity. *Advanced Drug Delivery Reviews* 61, 457-466.

Al-Qadi, S., Grenha, A., Carrión-Recio, D., Seijo, B., Remuñán-López, C., 2012. Microencapsulated chitosan nanoparticles for pulmonary protein delivery: In vivo evaluation of insulin-loaded formulations. *Journal of Controlled Release* 157, 383-390.

Amidi, M., Romeijn, S.G., Borchard, G., Junginger, H.E., Hennink, W.E., Jiskoot, W., 2006. Preparation and characterization of protein-loaded N-trimethyl chitosan nanoparticles as nasal delivery system. *Journal of Controlled Release* 111, 107-116.

Amidi, M., Romeijn, S.G., Verhoef, J.C., Junginger, H.E., Bungener, L., Huckriede, A., Crommelin, D.J.A., Jiskoot, W., 2007. N-Trimethyl chitosan (TMC) nanoparticles loaded with influenza subunit antigen for intranasal vaccination: Biological properties and immunogenicity in a mouse model. *Vaccine* 25, 144-153.

Antosova, Z., Mackova, M., Kral, V., Macek, T., 2009. Therapeutic application of peptides and proteins: parenteral forever? *Trends Biotechnol* 27, 628-635.

Artursson, P., Lindmark, T., Davis, S.S., Illum, L., 1994. Effect of chitosan on the permeability of monolayers of intestinal epithelial cells (Caco-2). *Pharmaceutical Research* 11, 1358-1361.

Beneke, C., Viljoen, A., Hamman, J., 2009. Polymeric plant-derived excipients in drug delivery. *Molecules* 14, 2602-2620.

Bhattacharjee, S., de Haan, L., Evers, N., Jiang, X., Marcelis, A., Zuilhof, H., Rietjens, I., Alink, G., 2010. Role of surface charge and oxidative stress in cytotoxicity of organic monolayer-coated silicon nanoparticles towards macrophage NR8383 cells. *Particle and Fibre Toxicology* 7, 2-12.

Bogataj, M., Vovk, T., Kerec, M., Dimnik, A., scaron, Grabnar, I., Mrhar, A., 2003. The correlation between zeta potential and mucoadhesion strength on pig vesical mucosa. *Biological and Pharmaceutical Bulletin* 26, 743-746.

Borchard, G., Lueßen, H.L., de Boer, A.G., Verhoef, J.C., Lehr, C.-M., Junginger, H.E., 1996. The potential of mucoadhesive polymers in enhancing intestinal peptide drug absorption. III: Effects of chitosan-glutamate and carbomer on epithelial tight junctions in vitro. *Journal of Controlled Release* 39, 131-138.

Boridy, S., Takahashi, H., Akiyoshi, K., Maysinger, D., 2009. The binding of pullulan modified cholesteryl nanogels to A β oligomers and their suppression of cytotoxicity. *Biomaterials* 30, 5583-5591.

Calvo, P., Remuñán-López, C., Vila-Jato, J.L., Alonso, M.J., 1997a. Chitosan and chitosan/ethylene oxide-propylene oxide block copolymer nanoparticles as novel carriers for proteins and vaccines. *Pharmaceutical Research* 14, 1431-1436.

Calvo, P., Remuñán-López, C., Vila-Jato, J.L., Alonso, M.J., 1997b. Novel hydrophilic chitosan-polyethylene oxide nanoparticles as protein carriers. *Journal of Applied Polymer Science* 63, 125-132.

Carvalho, F., Bruschi, M., Evangelista, R., Gremião, M., 2010. Mucoadhesive drug delivery systems. *Brazilian Journal of Pharmaceutical Sciences* 46, 1-17.

Casettari, L., Villasaliu, D., Mantovani, G., Howdle, S.M., Stolnik, S., Illum, L., 2010. Effect of PEGylation on the toxicity and permeability enhancement of chitosan. *Biomacromolecules* 11, 2854-2865.

Chacon, M., Molpeceres, J., Berges, L., Guzman, M., Aberturas, M.R., 1999. Stability and freeze-drying of cyclosporine loaded poly(D,L lactide-glycolide) carriers. *European Journal of Pharmaceutical Sciences* 8, 99-107.

Chen, F., Zhang, Z.R., Yuan, F., Qin, X., Wang, M., Huang, Y., 2008. In vitro and in vivo study of N-trimethyl chitosan nanoparticles for oral protein delivery. *International Journal of Pharmaceutics* 349, 226-233.

Chen, K., Xu, Y., Rana, S., Miranda, O.R., Dubin, P.L., Rotello, V.M., Sun, L., Guo, X., 2011. Electrostatic selectivity in protein–nanoparticle interactions. *Biomacromolecules* 12, 2552-2561.

Cheng, K.-C., Demirci, A., Catchmark, J., 2011. Pullulan: biosynthesis, production, and applications. *Applied Microbiology and Biotechnology* 92, 29-44.

Chiellini, F., Piras, A.M., Errico, C., Chiellini, E., 2008. Micro/nanostructured polymeric systems for biomedical and pharmaceutical applications. *Nanomedicine* 3, 367-393.

Constantin, M., Fundueanu, G., Cortesi, R., Esposito, E., Nastruzzi, C., 2003. Aminated polysaccharide microspheres as DNA delivery systems. *Drug Delivery* 10, 138-149.

Cooper, C., Dubin, P., Kayitmazer, A., Turksen, S., 2005. Polyelectrolyte–protein complexes. *Current Opinion in Colloid and Interface Science* 10, 52-78.

De Campos, A.M., Sánchez, A., Alonso, M.a.J., 2001. Chitosan nanoparticles: a new vehicle for the improvement of the delivery of drugs to the ocular surface. Application to cyclosporin A. *International Journal of Pharmaceutics* 224, 159-168.

de la Fuente, M., Csaba, N., Garcia-Fuentes, M., Alonso, M.J., 2008a. Nanoparticles as protein and gene carriers to mucosal surfaces. *Nanomedicine* 3, 845-857.

de la Fuente, M., Seijo, B., Alonso, M.J., 2008b. Novel hyaluronan-based nanocarriers for transmucosal delivery of macromolecules. *Macromolecular Bioscience* 8, 441-450.

Desai, M.P., Labhasetwar, V., Amidon, G.L., Levy, R.J., 1996. Gastrointestinal uptake of biodegradable microparticles: effect of particle size. *Pharmaceutical Research* 13, 1838-1845.

Dionísio, M., Rosa da Costa, A., Soares, S., Grenha, A., 2011. Modified pullulan-based nanoparticles for protein delivery, Proceedings of 3rd PharmSciFair, Prague, Czech Republic.

Dornish, M., Hagen, A., Hansson, E., Peucheur, C., Vedier, F., Skaugrud, O., 1997. Safety of Protasan: ultrapure chitosan salts for biomedical and pharmaceutical use, in: Domard, A., Roberts, G., Varum, K. (Eds.), Advances in chitin science. Jacques Andre Publisher, Lyon, pp. 664-670.

Fernández-Urrusuno, R., Calvo, P., Remuñán-López, C., Vila-Jato, J.L., José Alonso, M., 1999a. Enhancement of nasal absorption of insulin using chitosan nanoparticles. *Pharmaceutical Research* 16, 1576-1581.

Fernández-Urrusuno, R., Romani, D., Calvo, P., Vila-Jato, J.L., Alonso, M.J., 1999b. Development of a freeze-dried formulation of insulin-loaded chitosan nanoparticles intended for nasal administration. *STP Pharma Sciences* 9, 429-436.

Freixeiro, P., Diéguez-Casal, E., Costoya, L., Seijo, B., Ferreirós, C.M., Criado, M.T., Sánchez, S., 2013. Study of the stability of proteoliposomes as vehicles for vaccines against *Neisseria meningitidis* based on recombinant porin complexes. *International Journal of Pharmaceutics* 443, 1-8.

Gan, Q., Wang, T., 2007. Chitosan nanoparticle as protein delivery carrier - Systematic examination of fabrication conditions for efficient loading and release. *Colloids and Surfaces B: Biointerfaces* 59, 24-34.

Gao, F., Cai, Y., Zhou, J., Xie, X., Ouyang, W., Zhang, Y., Wang, X., Zhang, X., Wang, X., Zhao, L., Tang, J., 2010. Pullulan acetate coated magnetite nanoparticles for hyperthermia: Preparation, characterization and in vitro experiments. *Nano Research* 3, 23-31.

Gaspar, R., Duncan, R., 2009. Polymeric carriers: Preclinical safety and the regulatory implications for design and development of polymer therapeutics. *Advanced Drug Delivery Reviews* 61, 1220-1231.

Goycoolea, F.M., Lollo, G., Remunan-Lopez, C., Quaglia, F., Alonso, M.J., 2009. Chitosan-alginate blended nanoparticles as carriers for the transmucosal delivery of macromolecules. *Biomacromolecules* 10, 1736-1743.

Grainger, C., Greenwell, L., Lockley, D., Martin, G., Forbes, B., 2006. Culture of Calu-3 cells at the air interface provides a representative model of the airway epithelial barrier. *Pharmaceutical Research* 23, 1482-1490.

Grenha, A., 2012. Chitosan nanoparticles: a survey of preparation methods. *Journal of Drug Targeting* 20, 291-300.

Grenha, A., Al-Qadi, S., Seijo, B., Remuñán-López, C., 2010a. The potential of chitosan for pulmonary drug delivery. *Journal of Drug Delivery Sciences and Technology* 20, 33-43.

Grenha, A., Gomes, M.E., Rodrigues, M., Santo, V.E., Mano, J.F., Neves, N.M., Reis, R.L., 2010b. Development of new chitosan/carrageenan nanoparticles for drug delivery applications. *Journal of Biomedical Materials Research Part A* 92A, 1265-1272.

Grenha, A., Seijo, B., Remuñán-López, C., 2005. Microencapsulated chitosan nanoparticles for lung protein delivery. *European Journal of Pharmaceutical Sciences* 25, 427-437.

Grenha, A., Seijo, B., Serra, C., Remuñán-López, C., 2007. Chitosan nanoparticle-loaded mannitol microspheres: Structure and surface characterization. *Biomacromolecules* 8, 2072-2079.

Gupta, A.K., Gupta, M., 2005. Cytotoxicity suppression and cellular uptake enhancement of surface modified magnetic nanoparticles. *Biomaterials* 26, 1565-1573.

Gupta, M., Gupta, A., 2004a. In vitro cytotoxicity studies of hydrogel pullulan nanoparticles prepared by aot/n-hexane micellar system. *Journal of Pharmacy and Pharmaceutical Sciences* 7, 38-46.

Gupta, M., Gupta, A.K., 2004b. Hydrogel pullulan nanoparticles encapsulating pBUDLacZ plasmid as an efficient gene delivery carrier. *Journal of Controlled Release* 99, 157-166.

Hafner, A., Lovrić, J., Voinovich, D., Filipović-Grčić, J., 2009. Melatonin-loaded lecithin/chitosan nanoparticles: Physicochemical characterisation and permeability through Caco-2 cell monolayers. *International Journal of Pharmaceutics* 381, 205-213.

Hartig, S., Greene, R., Dikov, M., Prokop, A., Davidson, J., 2007. Multifunctional nanoparticulate polyelectrolyte complexes. *Pharmaceutical Research* 24, 2353-2369.

Hassani, L., Hendra, F., Bouchemal, K., 2012. Auto-associative amphiphilic polysaccharides as drug delivery systems. *Drug Discovery Today* 17, 608-614.

Hirano, S., Seino, H., Akiyama, Y., Nonaka, I., 1988. Bio-compatibility of chitosan by oral and intravenous administrations. *Polymeric Materials Science and Engineering* 59, 897-901.

Hirsjärvi, S., Peltonen, L., Hirvonen, J., 2009. Effect of sugars, surfactant, and tangential flow filtration on the freeze-drying of poly(lactic acid) nanoparticles. *AAPS PharmSciTech* 10, 488-494.

Hofmann, W., Asgharian, B., 2003. The effect of lung structure on mucociliary clearance and particle retention in human and rat lungs. *Toxicological Sciences* 73, 448-456.

Ikeda, S., Zhong, Q., 2012. Polymer and colloidal models describing structure-function relationships. *Annual Review of Food Science and Technology* 3, 405-424.

Iinskaya, O., Dreyer, F., Mitkevich, V., Shaw, K., Pace, C., Makarov, A., 2002. Changing the net charge from negative to positive makes ribonuclease Sa cytotoxic. *Protein Science* 11, 2522-2525.

Illum, L., 2002. Nasal drug delivery: new developments and strategies. *Drug Discovery Today* 7, 1184-1189.

ISO, 2003. Biological evaluation of medical devices Part 3: Tests for genotoxicity, carcinogenicity, and reproductive toxicity, in: *Standardization, I.O.f. (Ed.)*, 10993-3.

ISO, 2009a. Biological evaluation of medical devices Part 1: Evaluation and testing, in: *Standardization, I.O.f. (Ed.)*, 10993-1.

ISO, 2009b. Biological evaluation of medical devices Part 5: Tests for in vitro cytotoxicity, in: *Standardization, I.O.f. (Ed.)*, 10993-5.

Janes, K.A., Calvo, P., Alonso, M.J., 2001. Polysaccharide colloidal particles as delivery systems for macromolecules. *Advanced Drug Delivery Reviews* 47, 83-97.

Jani, P., Halbert, G., Langridge, J., Florence, A., 1990. Nanoparticle uptake by the rat gastrointestinal mucosa: quantitation and particle size dependency. *Journal of Pharmacy and Pharmacology* 42, 821-826.

Jeong, Y.-I., Nah, J.-W., Na, H.-K., Na, K., Kim, I.-S., Cho, C.-S., Kim, S.-H., 1999. Self-assembling nanospheres of hydrophobized pullulans in water. *Drug Development and Industrial Pharmacy* 25, 917-927.

Karewicz, A., Bielska, D., Nowakowska, M., 2012. Modified polysaccharides as versatile materials in controlled delivery of anti-degenerative agents. *Current Pharmaceutical Design* 18, 2518-2535.

Kumar, G., Shafiq, N., Malhotra, S., 2012. Drug-loaded PLGA nanoparticles for oral administration: fundamental issues and challenges ahead. *Critical Reviews in Therapeutic Drug Carrier Systems* 29, 149-182.

Lansley, A., Martin, G.P., 2001. Nasal drug delivery, in: Hillery, A.M., Lloyd, A.W., Swarbrick, J. (Eds.), *Drug Delivery and Targeting: For Pharmacists and Pharmaceutical Scientists*. Taylor & Francis, London, pp. 237-268.

Leathers, T.D., 2003. Biotechnological production and applications of pullulan. *Applied Microbiology and Biotechnology* 62, 468-473.

Lee, S.J., Hong, G.-Y., Jeong, Y.-I., Kang, M.-S., Oh, J.-S., Song, C.-E., Lee, H.C., 2012. Paclitaxel-incorporated nanoparticles of hydrophobized polysaccharide and their antitumor activity. *International Journal of Pharmaceutics* 433, 121-128.

Lehr, C.-M., Bouwstra, J.A., Schacht, E.H., Junginger, H.E., 1992. In vitro evaluation of mucoadhesive properties of chitosan and some other natural polymers. *International Journal of Pharmaceutics* 78, 43-48.

Li, S., Patapoff, T., Overcashier, D., Hsu, C., Nguyen, T., Borchardt, R., 1996. Effects of reducing sugars on the chemical stability of human relaxin in the lyophilized state. *Journal of Pharmaceutical Sciences* 85, 873-877.

Liu, Z., Jiao, Y., Liu, F., Zhang, Z., 2007. Heparin/chitosan nanoparticle carriers prepared by polyelectrolyte complexation. *Journal of Biomedical Materials Research Part A* 83A, 806-812.

Liu, Z., Jiao, Y., Wang, Y., Zhou, C., Zhang, Z., 2008. Polysaccharides-based nanoparticles as drug delivery systems. *Advanced Drug Delivery Reviews* 60, 1650-1662.

Malafaya, P., Silva, G., Reis, R., 2007. Natural-origin polymers as carriers and scaffolds for biomolecules and cell delivery in tissue engineering application. *Advanced Drug Delivery Reviews* 59, 207-233.

Meyres, L., Gamst, G., Guarino, A., 2012. *Applied multivariate research. Design and interpretation*, 2 ed. Sage.

Mizrahy, S., Peer, D., 2012. Polysaccharides as building blocks for nanotherapeutics. *The Chemistry Society Reviews* 41, 2623-2640.

Möller, W., Hauszinger, K., Ziegler-Heitbrock, L., Heyder, J., 2006. Mucociliary and long-term particle clearance in airways of patients with immotile cilia. *Respiratory Research* 7, 1-8.

Morris, G.A., Castile, J., Smith, A., Adams, G.G., Harding, S.E., 2011. The effect of prolonged storage at different temperatures on the particle size distribution of tripolyphosphate (TPP) – chitosan nanoparticles. *Carbohydrate Polymers* 84, 1430-1434.

Nakanishi, K., Goto, T., Ohashi, M., 1957. Infrared spectra of organic ammonium compounds. *Bulletin of the Chemical Society of Japan* 30, 403-408.

Namazi, H., Fathi, F., Heydari, A., 2011. Nanoparticles based on modified polysaccharides, *The delivery of nanoparticles*. Intech, pp. 149-184.

Nochi, T., Yuki, Y., Takahashi, H., Sawada, S.-i., Mejima, M., Kohda, T., Harada, N., Kong, I.G., Sato, A., Kataoka, N., Tokuhara, D., Kurokawa, S., Takahashi, Y., Tsukada, H., Kozaki, S., Akiyoshi, K., Kiyono, H., 2010. Nanogel antigenic protein-delivery system for adjuvant-free intranasal vaccines. *Nat Mater* 9, 572-578.

Oyarzun-Ampuero, F., Brea, J., Loza, M., Torres, D., Alonso, M.J., 2009. Chitosan-hyaluronic acid nanoparticles loaded with heparin for the treatment of asthma. *International Journal of Pharmaceutics* 381, 122-129.

Portero, A., Remuñán-López, C., Nielsen, H.M., 2002. The potential of chitosan in enhancing peptide and protein absorption across the TR146 cell culture model — An in vitro model of the buccal epithelium. *Pharmaceutical Research* 19, 169-174.

Pouliot, J.M., Walton, I., Nolen-Parkhouse, M., Abu-Lail, L.I., Camesano, T.A., 2005. Adhesion of *Aureobasidium pullulans* is controlled by uronic acid based polymers and pullulan. *Biomacromolecules* 6, 1122-1131.

Prego, C., García, M., Torres, D., Alonso, M.J., 2005a. Transmucosal macromolecular drug delivery. *Journal of Controlled Release* 101, 151-162.

Prego, C., Torres, D., Alonso, M.J., 2005b. The potential of chitosan for the oral administration of peptides. *Expert Opinion on Drug Delivery* 2, 843-854.

Rekha, M., Chandra, P., 2007. Pullulan as a promising biomaterial for biomedical applications: A perspective. *Trends in Biomaterials and Artificial Organs* 20, 000-000.

Rinaudo, M., 2008. Main properties and current applications of some polysaccharides as biomaterials. *Polym. Int.* 57, 397-430.

Rodrigues, S., Dionísio, M., Remuñán-López, C., Grenha, A., 2012a. Biocompatibility of chitosan carriers with application in drug delivery. *Journal of Functional Biomaterials* 3, 615-641.

Rodrigues, S., Rosa da Costa, A., Grenha, A., 2012b. Chitosan/carrageenan nanoparticles: Effect of cross-linking with tripolyphosphate and charge ratios. *Carbohydrate Polymers* 89, 282-289.

Sakono, M., Zako, T., 2010. Amyloid oligomers: formation and toxicity of A β oligomers. *FEBS Journal* 277, 1348-1358.

Sameti, M., Bohr, G., Ravi Kumar, M.N.V., Kneuer, C., Bakowsky, U., Nacken, M., Schmidt, H., Lehr, C.M., 2003. Stabilisation by freeze-drying of cationically modified silica nanoparticles for gene delivery. *International Journal of Pharmaceutics* 266, 51-60.

Sarmento, B., Ribeiro, A., Veiga, F., Ferreira, D., 2006. Development and characterization of new insulin containing polysaccharide nanoparticles. *Colloids and Surfaces B: Biointerfaces* 53, 193-202.

Scherließ, R., 2011. The MTT assay as tool to evaluate and compare excipient toxicity in vitro on respiratory epithelial cells. *International Journal of Pharmaceutics* 411, 98-105.

Seyrek, E., Dubin, P., Tribet, C., Gamble, E., 2003. Ionic strength dependence of protein-polyelectrolyte interactions. *Biomacromolecules* 4, 273-282.

Shimizu, T., Kishida, T., Hasegawa, U., Ueda, Y., Imanishi, J., Yamagishi, H., Akiyoshi, K., Otsuji, E., Mazda, O., 2008. Nanogel DDS enables sustained release of IL-12 for tumor immunotherapy. *Biochemical and Biophysical Research Communications* 367, 330-335.

Simkovic, I., Yadav, M.P., Zalibera, M., Hicks, K.B., 2009. Chemical modification of corn fiber with ion-exchanging groups. *Carbohydrate Polymers* 76, 250-254.

Team, R.C., 2013. R: A language and environment for statistical computing. R Foundation for Statistical Computing, Vienna, Austria.

- , C., Alonso, M., 2009. New generation of hybrid poly/oligosaccharide nanoparticles as carriers for the nasal delivery of macromolecules. *Biomacromolecules* 10, 243-249.

Teramoto, N., Shibata, M., 2006. Synthesis and properties of pullulan acetate. Thermal properties, biodegradability, and a semi-clear gel formation in organic solvents. *Carbohydrate Polymers* 63, 476-481.

Turcotte, R.F., Lavis, L.D., Raines, R.T., 2009. Onconase cytotoxicity relies on the distribution of its positive charge. *The FEBS journal* 276, 3846-3857.

Vandana, M., Sahoo, S.K., 2009. Optimization of physicochemical parameters influencing the fabrication of protein-loaded chitosan nanoparticles. *Nanomedicine* 4, 773-785.

Vauthier, C., Bouchemal, K., 2009. Methods for the preparation and manufacture of polymeric nanoparticles. *Pharmaceutical Research* 26, 1025-1058.

Walters, D.V., 2002. Lung lining liquid – The hidden depths. *Neonatology* 81, 2-5.

Wang, W., 2000. Lyophilization and development of solid protein pharmaceuticals. *International Journal of Pharmaceutics* 203, 1-60.

Williams, D.F., 2008. On the mechanisms of biocompatibility. *Biomaterials* 29, 2941-2953.

Wilson, R., Smith, A., Kacurakova, M., Saunders, P., Wellner, N., Waldron, K., 2000. The mechanical properties and molecular dynamics of plant cell wall polysaccharides studied by Fourier-transform infrared spectroscopy. *Plant Physiology* 124, 397-405.

Wu, L., Zhang, J., Watanabe, W., 2011. Physical and chemical stability of drug nanoparticles. *Adv Drug Deliv Rev* 63, 456-469.

Xu, Y., Du, Y., Huang, R., Gao, L., 2003. Preparation and modification of N-(2-hydroxyl) propyl-3-trimethyl ammonium chitosan chloride as a protein carrier. *Biomaterials* 24, 5015-5022.

Yamamoto, H., Kuno, Y., Sugimoto, S., Takeuchi, H., Kawashima, Y., 2005. Surface-modified PLGA nanosphere with chitosan improved pulmonary delivery of calcitonin by mucoadhesion and opening of the intercellular tight junctions. *Journal of Controlled Release* 102, 373-381.

Yampolskaya, G., Platikanov, D., 2006. Proteins at fluid interfaces: Adsorption layers and thin liquid films. *Advances in Colloid and Interface Science* 128–130, 159-183.

Yuan, H., Zhang, W., Li, X., Lu, X., Li, N., Gao, X., Song, J., 2005. Preparation and in vitro antioxidant activity of k-carrageenan oligosaccharides and their oversulfated, acetylated, and phosphorylated derivatives. *Carbohydrate Research* 340, 685-692.

Zhu, Y., Chidekel, A., Shaffer, T., 2010. Cultured human airway epithelial cells (Calu-3): A model of human respiratory function, structure, and inflammatory responses. *Critical Care Research and Practice* 2010, 1-8.

Zobel, H.P., Stieneker, F., Atmaca-Abdel Aziz, S., Gilbert, M., Werner, D., R. Noe, C., Kreuter, J., Zimmer, A., 1999. Evaluation of aminoalkylmethacrylate nanoparticles as colloidal drug carrier systems. Part II: characterization of antisense oligonucleotides loaded copolymer nanoparticles. *European Journal of Pharmaceutics and Biopharmaceutics* 48, 1-12.

Zorzi, G.K., Párraga, J.E., Seijo, B., Sánchez, A., 2011. Hybrid nanoparticle design based on cationized gelatin and the polyanions dextran sulfate and chondroitin sulfate for ocular gene therapy. *Macromolecular Bioscience* 11, 905-913.

Figure captions

Figure 1. A) Chemical structures of chitosan (CS), *k*-carrageenan (CRG) and pullulan derivatives, B) FTIR spectra of CS, sulfated pullulan (SP), SP/CS nanoparticles, bovine serum albumin (BSA)-loaded SP/CS nanoparticles and BSA; and C) CRG, aminated pullulan (AP), CRG/AP nanoparticles, BSA-loaded CRG/AP nanoparticles and BSA.

Figure 2. TEM microphotographs of pullulan-based nanoparticles: A) nanoparticles SP/CS = 1/2 and B) nanoparticles CRG/AP = 1/2.

Figure 3. *In vitro* release of BSA from (▲) SP/CS nanoparticles and (■) CRG/AP nanoparticles assessed in PBS pH 7.4 at 37 °C (mean ± S.D., n = 3).

Figure 4. Size variation of A) CRG/AP = 1/2 and B) SP/CS = 1/2 nanoparticles, upon freeze-drying in presence of sucrose (black), lactose (dark grey), trehalose (light grey) and glucose (white), and further reconstitution in water (hydrodynamic diameter of nanoparticles before (Di) and after (Df) freeze-drying) (mean ± S.D., n = 3).

Figure 5. Half normal plots of the effects obtained from the factorial design of the assay variables: time (X_1), concentration (X_2) and type of polymer/nanoparticles (X_3), on Calu-3 cells viability. A) Polymers and B) Nanoparticles (* indicates the statistically significant effects).

Figure 6. Calu-3 cell viability measured by MTT assay after A) 3h and B) 24h exposure to increasing concentrations of (◆) chitosan, (■) carrageenan, (●) unmodified pullulan,

(▲) sulfated pullulan and (×) aminated pullulan. Data represent mean \pm S.E.M. (n = 3, six replicates per experiment at each concentration).

Figure 7. Calu-3 cell viability measured by MTT assay after 3h (empty symbols) and 24h (black symbols) exposure to increasing concentrations of (□) SP/CS nanoparticles and (○) CRG/AP nanoparticles. Data represent mean \pm S.E.M. (n = 3, six replicates per experiment at each concentration).

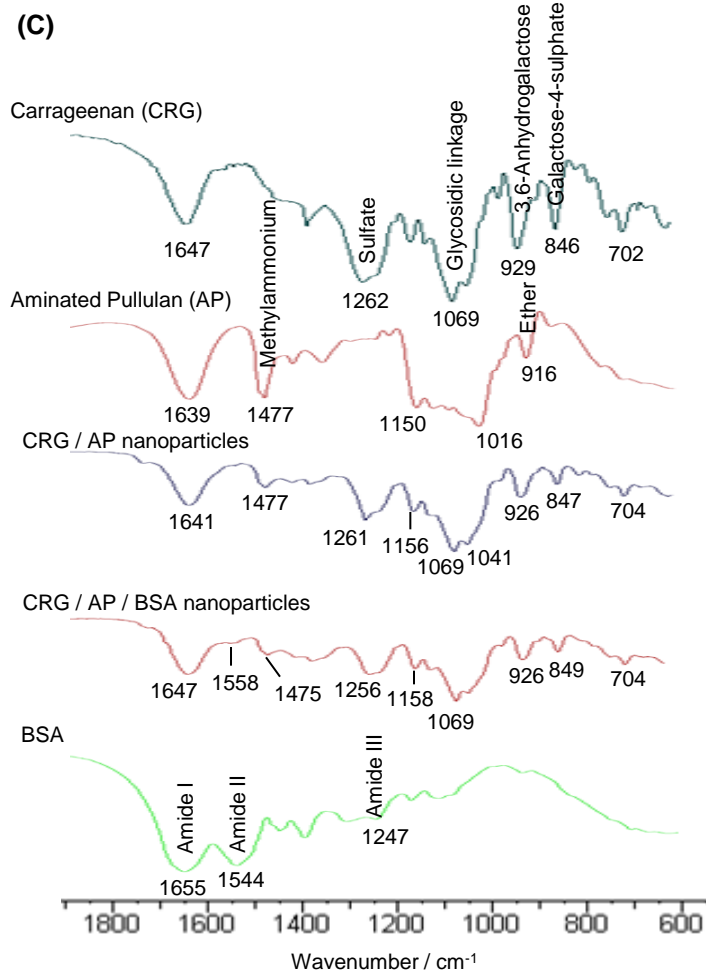
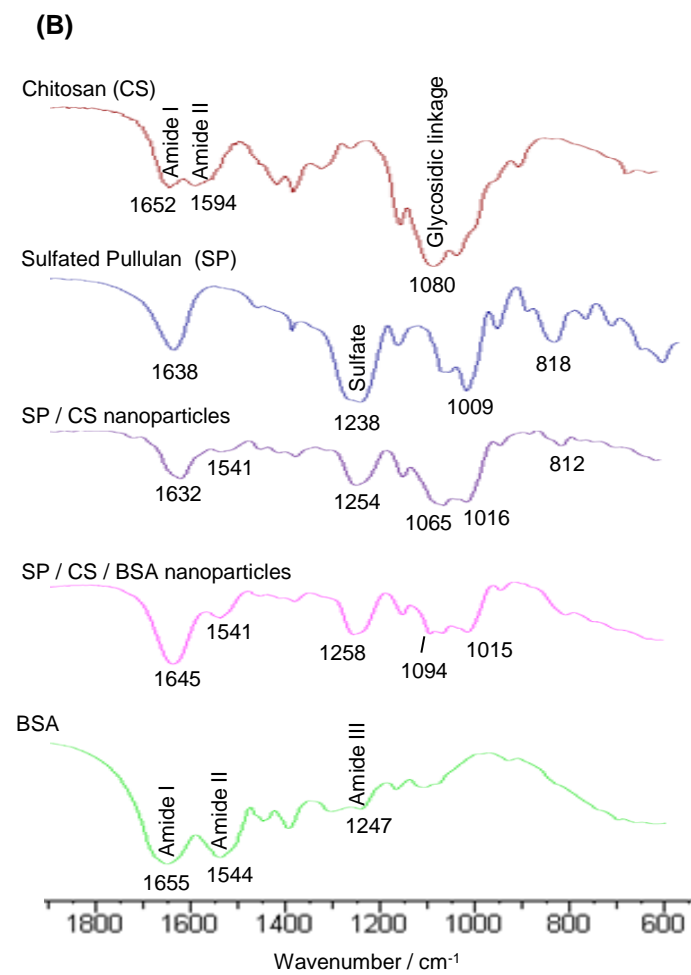
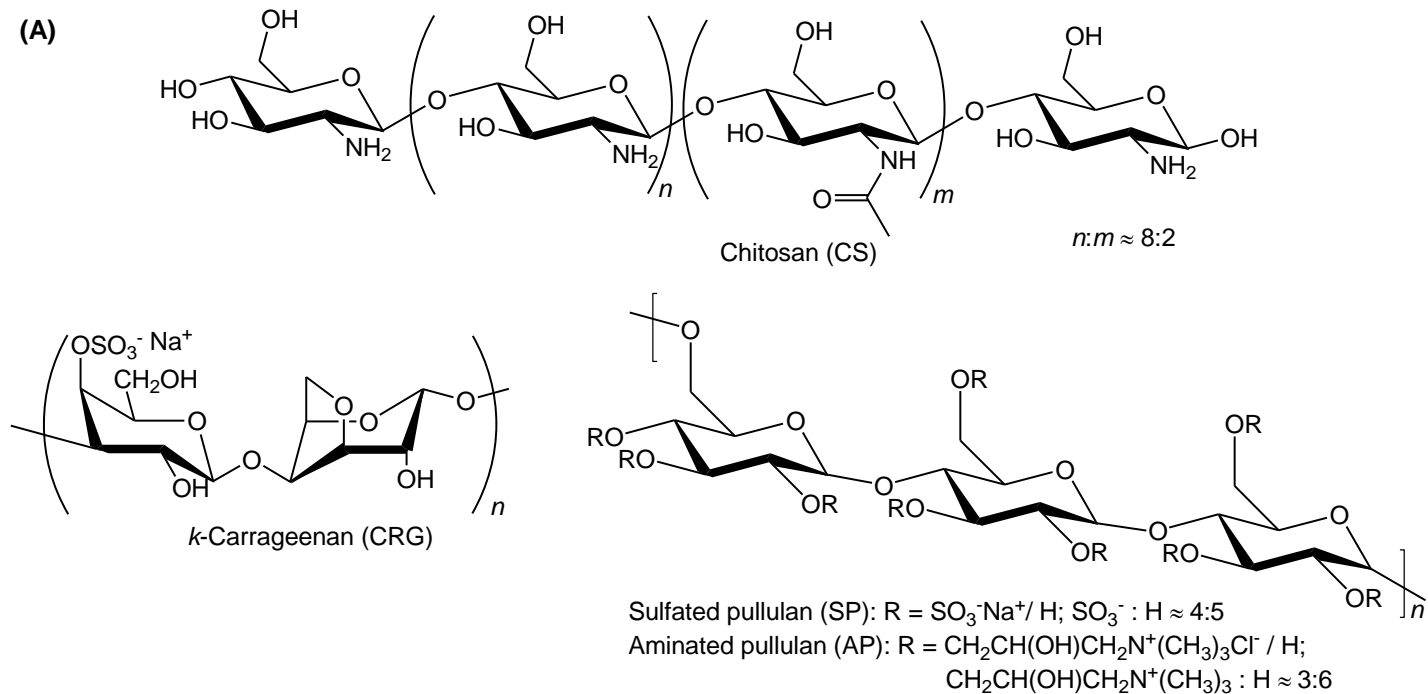
Figure 1

Figure 2

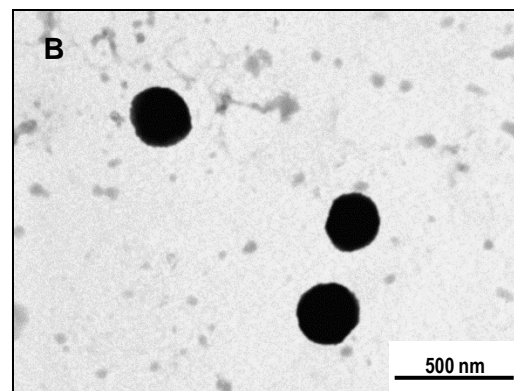
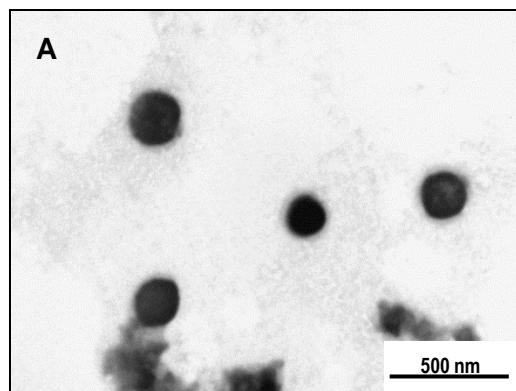


Figure 3

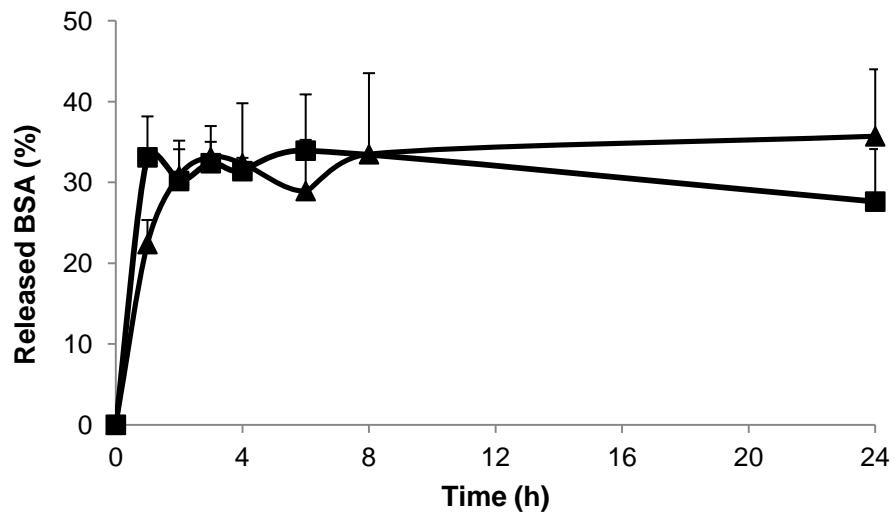


Figure 4

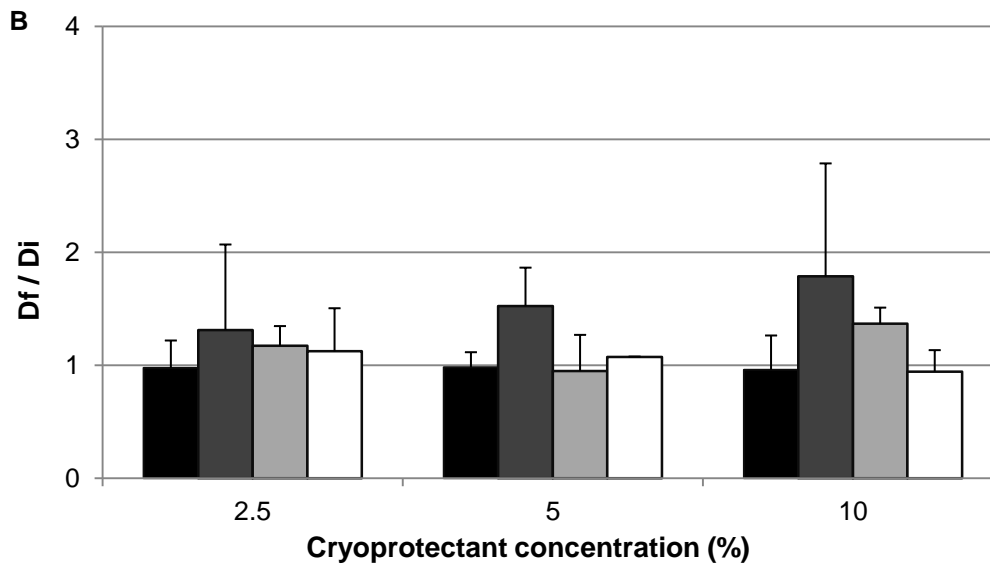
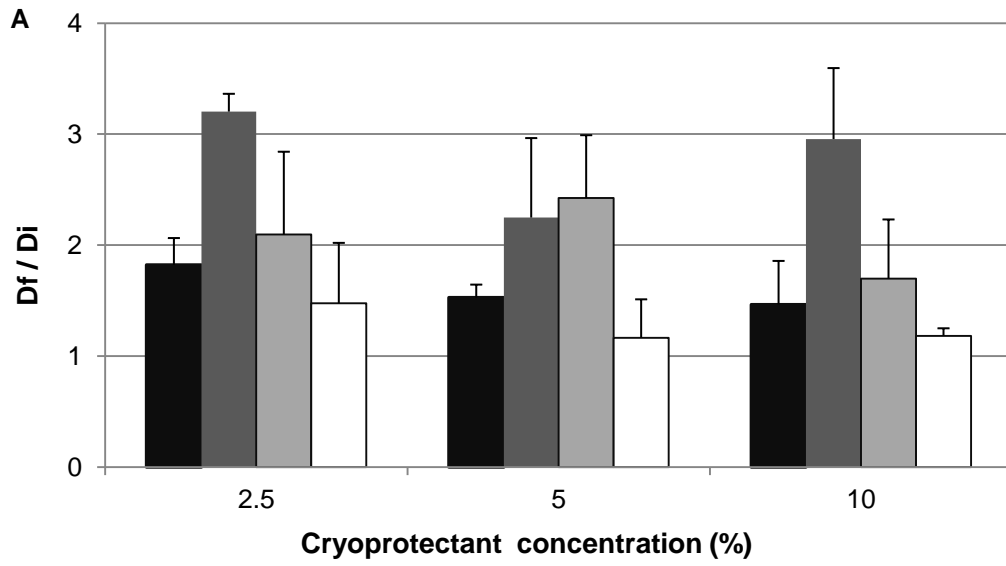


Figure 5
[Click here to download high resolution image](#)

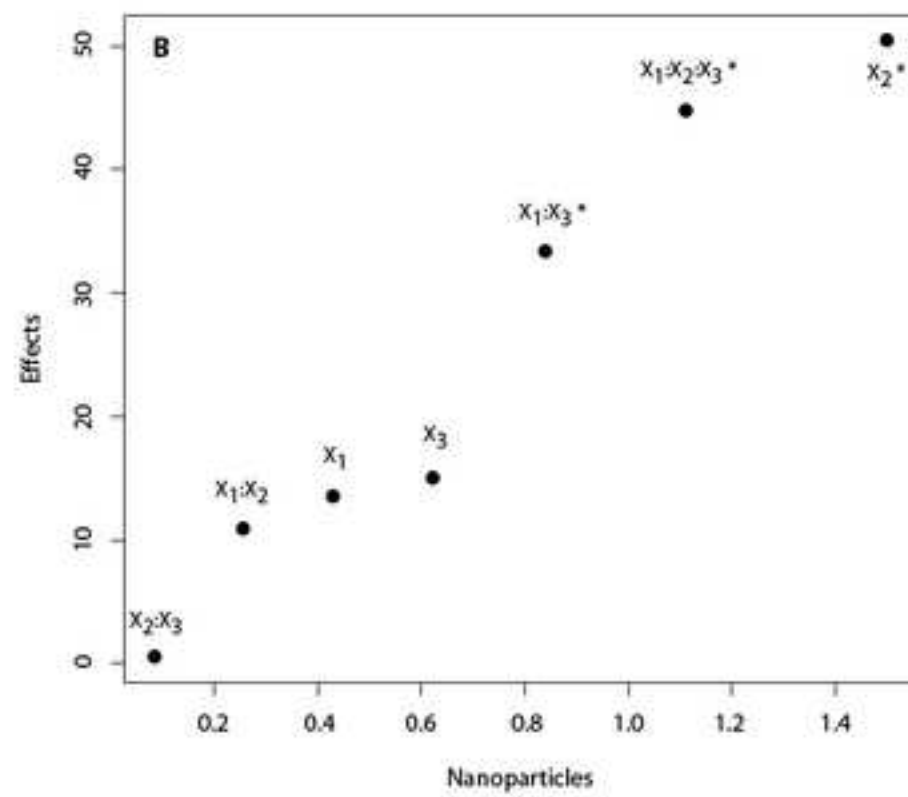
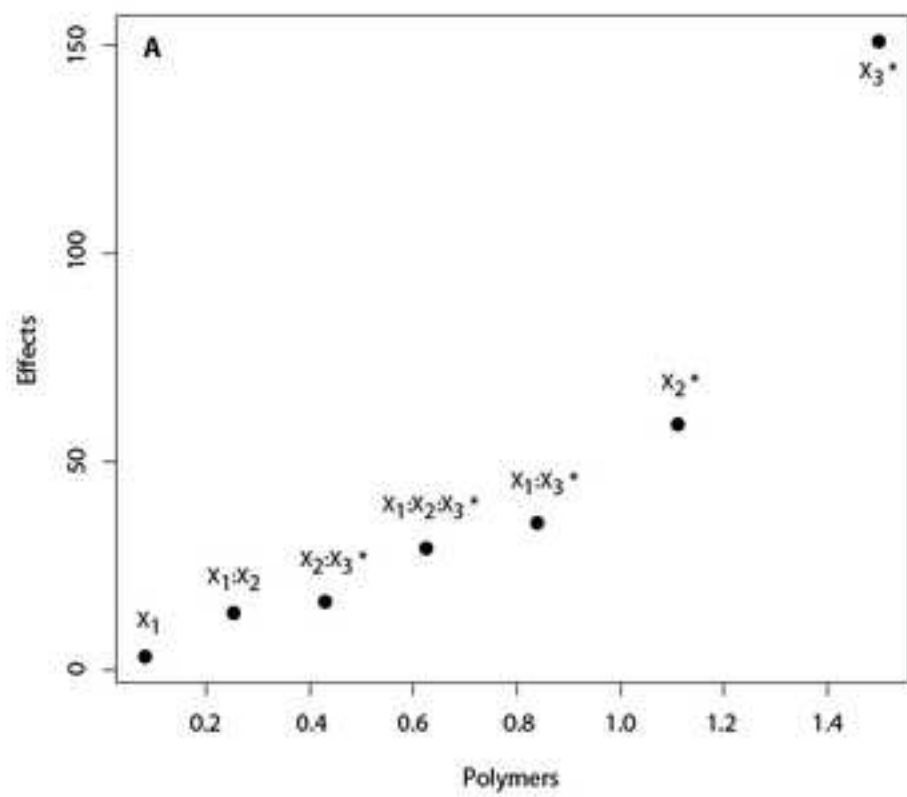


Figure 6

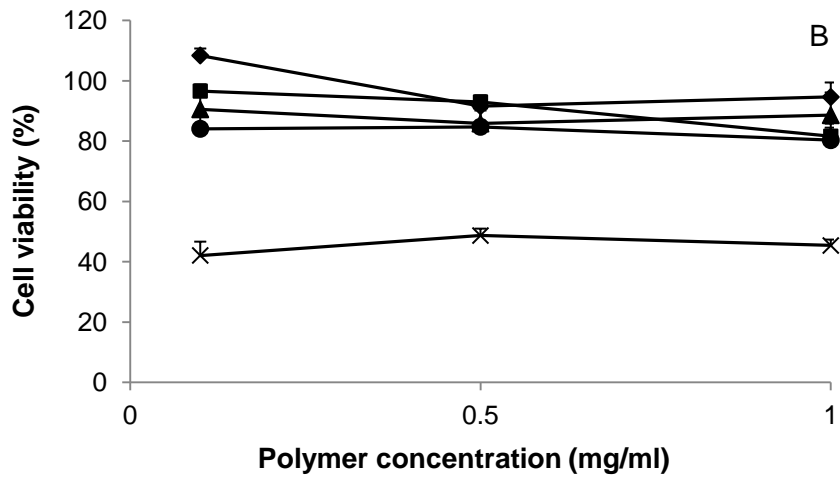
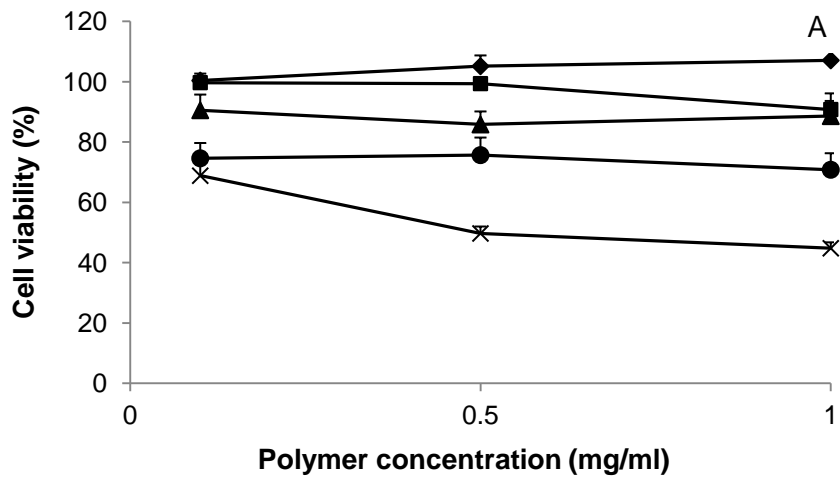


Figure 7

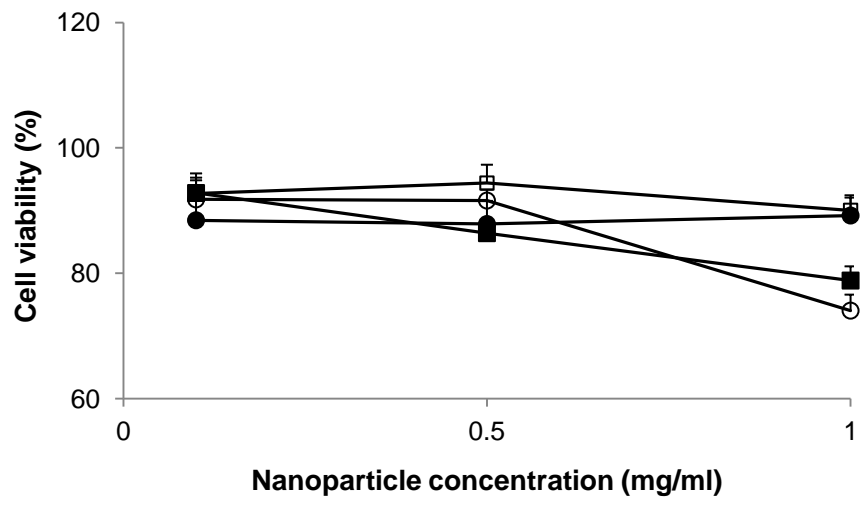


Table 1. Physicochemical characteristics, production yield and bovine serum albumin encapsulation efficiency of pullulan-based nanoparticles (mean \pm S.D., n = 3).

Nanoparticle formulation	Size (nm)	ζ-potential (mV)	Production yield (%)	Encapsulation efficiency (%)	Loading capacity (%)
SP/CS = 1/2 Unloaded	261 \pm 42	+ 50 \pm 7	26 \pm 9	—	—
SP/CS = 1/2 BSA-loaded	271 \pm 50	+ 50 \pm 9	28 \pm 8	44 \pm 13	30 \pm 8
CRG/AP = 1/2 Unloaded	185 \pm 44	+ 56 \pm 9	18 \pm 8	—	—
CRG/AP = 1/2 BSA-loaded	244 \pm 50	+ 58 \pm 8	19 \pm 9	34 \pm 7	31 \pm 6

AP: aminated pullulan; BSA: bovine serum albumin; CRG: carrageenan; CS: chitosan; SP: sulfated pullulan